Spectral and temporal distribution of phase-conjugated fluorescent photons

HENK F. ARNOLDUS

Department of Physics, Mendel Hall, Villanova University,
Villanova, Pennsylvania 19085, USA

and THOMAS F. GEORGE

Departments of Chemistry and Physics & Astronomy,
239 Fronczak Hall, State University of New York at Buffalo,
Buffalo, New York 14260, USA

Abstract. Spontaneous emission of fluorescence radiation by an atom near the surface of a four-wave mixing phase conjugator is considered. It is shown that the spectral photon distribution consists of two Lorentzians, which have their peaks symmetrically located at the two sides of the pump frequency $\bar{\omega}$ of the nonlinear crystal. With ω_0 the atomic resonance, the line at $2\bar{\omega} - \omega_0$ is more than twice as strong as the line at ω_0. When the phase-conjugate reflectivity exceeds unity, the temporal photon distribution exhibits nonclassical behaviour. Then, antibunching of photons prevails, and the photon statistics are sub-Poissonian.

1. Introduction

When two strong counterpropagating laser beams with frequency $\bar{\omega}$ pump a nonlinear crystal, then this device operates as a phase conjugator (PC) for weak incident radiation on its surface, as a result of a four-wave mixing process in the medium. In particular, the electromagnetic vacuum field interacts with the pump beams, resulting in a spontaneous emission of photons with frequency $\bar{\omega}$ in all directions [1]. When a two-state atom with level separation $\hbar\omega_0$ is located in the vicinity of the surface of the PC, it can absorb these photons. This leads to spontaneous excitation of the atom [2, 3] through a three-photon process, as illustrated in figure 1. An atom in its ground state $|g\rangle$ absorbs a photon with frequency $\bar{\omega}$, and subsequently emits spontaneously a photon with frequency $2\bar{\omega} - \omega_0$. The energy-conserving diagram is completed by a second absorption of a photon with frequency $\bar{\omega}$, which leaves the atom in the excited state $|e\rangle$. This process is reminiscent of the generation of the three-photon line in resonance fluorescence by an atom in a laser field with frequency $\bar{\omega}$ [4]. After this excitation, the atom decays spontaneously in the usual way, which produces a photon with frequency ω_0. Continuous repetition of this cycle should lead to a steady emission of photons with frequencies ω_0 and $2\bar{\omega} - \omega_0$.

The above interpretation of spontaneous emission by an atom near a PC is simply based on energy conservation. We shall show that the fluorescence spectrum consists indeed of two lines, which are positioned at ω_0 and $2\bar{\omega} - \omega_0$. Furthermore, we shall evaluate the two-photon correlation function. The antibunching between two ω_0-photons and between two $2\bar{\omega} - \omega_0$-photons then reveals the alternating character of the two emission mechanisms from figure 1.
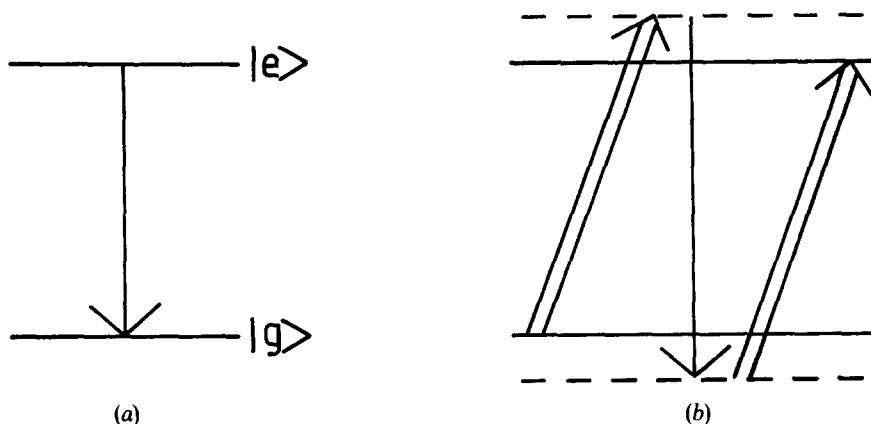
H. F. Arnoldus and T. F. George

Figure 1. Diagram (*a*) corresponds to ordinary spontaneous decay and the emission of a
photon with frequency ω_0. Diagram (*b*) represents a three-photon process. Two
photons with frequency $\bar{\omega}$ are absorbed (double lines), and the atom goes from the
ground state to the excited state. Therefore, the fluorescent photon which is emitted in
between the two absorptions must have a frequency $2\bar{\omega} - \omega_0$.

2. Fluorescence

The surface of the PC is taken as the xy-plane, and the atom with dipole moment
$\mu(t)$ is located on the positive z-axis at $z = h$. The positive-frequency part of the
fluorescence radiation field is given by [5]

$$E(r, t)^{(+)} = \omega_0^2 \frac{\exp(-i\omega_0 \tau)}{4\pi\varepsilon_0 rc^2} \{M(t) - \hat{r}(\hat{r} \cdot M(t))\}, \tag{1}$$

in the far zone. Here

$$\tau = (h/c) \cos \theta, \tag{2}$$

and the operator $M(t)$ is defined as

$$M(t) = \mu(t)^{(+)} - P^* \exp(-2i\bar{\omega}t)\mu(t)^{(-)}, \tag{3}$$

in terms of the positive- and negative-frequency parts of the dipole operator, and the
Fresnel reflection coefficient P for a plane wave with frequency ω_0. We have
suppressed the retardation with $-r/c$. Equation (1) was derived by solving the
Maxwell–Heisenberg equations for a dipole near the surface of a PC. The term
proportional to $\mu(t)^{(+)}$ is dipole radiation by an atom in empty space. This radiation
reflects at the surface, with reflection coefficient P, and this produces the second
term. Due to the phase conjugation, $\mu^{(+)}$ is reflected as $\mu^{(-)}$, and the factor
$\exp(-2i\bar{\omega}t)$ accounts for the two $\bar{\omega}$ photons in figure 1 (*b*).

We shall assume that the radiation passes a polarizer, which transmits the
e_d-component of the field (with $e_d^* \cdot e_d = 1$). This component is

$$\mathscr{E}(t)^{(+)} = E(r, t)^{(+)} \cdot e_d^* = \omega_0^2 \frac{\exp(-i\omega_0\tau)}{4\pi\varepsilon_0 rc^2} M(t) \cdot e_d^*, \tag{4}$$

where we used $\mathbf{e}_d^* \cdot \hat{\mathbf{r}} = 0$. A photomultiplier then counts photons from this filtered field. With $\boldsymbol{\mu}_{eg} = \langle e|\boldsymbol{\mu}|g\rangle$, assumed to be real, the field becomes

$$\mathscr{E}(t)^{(+)} = \omega_0^2 \frac{\exp(-\mathrm{i}\omega_0\tau)}{4\pi\varepsilon_0 rc^2} (\boldsymbol{\mu}_{eg} \cdot \mathbf{e}_d)^* \{d^\dagger(t) - P^* \exp(-2\mathrm{i}\bar{\omega}t)\, d(t)\}, \tag{5}$$

in terms of the atomic raising operator $d = |e\rangle\langle g|$ and lowering operator $d^\dagger = |g\rangle\langle e|$.

3. Equation of motion

The atomic density operator $\rho(t)$ obeys the Liouville equation

$$\mathrm{i}\frac{\mathrm{d}\rho}{\mathrm{d}t} = (L_a - \mathrm{i}\Gamma)\rho, \qquad \rho^\dagger = \rho, \qquad \mathrm{Tr}\,\rho = 1, \tag{6}$$

where L_a and Γ represent the free evolution and relaxation, respectively. With the atomic Hamiltonian given by

$$H_a = \hbar\omega_e P_e + \hbar\omega_g P_g, \tag{7}$$

in terms of the projectors $P_e = |e\rangle\langle e|$ and $P_g = |g\rangle\langle g|$ onto the excited state and ground state, respectively, the Liouvillian L_a becomes

$$L_a\sigma = \hbar^{-1}[H_a, \sigma] = \omega_0[P_e, \sigma]. \tag{8}$$

Here we used $P_e + P_g = 1$ and $\omega_0 = \omega_e - \omega_g$. Equation (8) defines the action of L_a on an arbitrary Hilbert-space operator σ, rather than on the density operator ρ only. The relaxation operator is [6]

$$\Gamma\sigma = \tfrac{1}{2}A_e\{P_e\sigma + \sigma P_e - 2d^\dagger\sigma d\} + \tfrac{1}{2}A_g\{P_g\sigma + \sigma P_g - 2d\sigma d^\dagger\}, \tag{9}$$

in terms of the relaxation constants for the excited state and ground state

$$A_e = A(1 + \tfrac{1}{2}|P|^2), \tag{10}$$

$$A_g = \tfrac{1}{2}A|P|^2, \tag{11}$$

respectively. The parameter A is the Einstein coefficient for spontaneous decay in empty space.

Of particular interest is the steady-state density operator $\bar{\rho} = \rho(t \to \infty)$, which is the solution of

$$(L_a - \mathrm{i}\Gamma)\bar{\rho} = 0, \qquad \bar{\rho}^\dagger = \bar{\rho}, \qquad \mathrm{Tr}\,\bar{\rho} = 1. \tag{12}$$

We readily find

$$\bar{\rho} = \bar{n}_e P_e + \bar{n}_g P_g, \tag{13}$$

in terms of the steady-state level populations

$$\bar{n}_e = \frac{\tfrac{1}{2}|P|^2}{1 + |P|^2}, \qquad \bar{n}_g = 1 - \bar{n}_e. \tag{14}$$

The finite population of the excited state is due to the occurrence of the three-photon process from figure 1. The transient solution $\rho(t)$, given an initial state $\rho(0)$, can also be easily found.

4. Fluorescence spectrum

The stationary distribution of photons in a field $\mathscr{E}(t)$ is in general given by

$$J(\omega) = \frac{\zeta}{\pi} \mathrm{Re} \int_0^\infty d\tau \exp{(i\omega\tau)} \langle \mathscr{E}(0)^{(-)} \mathscr{E}(\tau)^{(+)} \rangle, \tag{15}$$

where ω is the photon frequency and ζ is an efficiency constant (depending on the aperture of the detector, etc.). The spectrally-unresolved intensity is

$$I = \int d\omega \, J(\omega) = \zeta \langle \mathscr{E}(0)^{(-)} \mathscr{E}(0)^{(+)} \rangle, \tag{16}$$

which equals the photon counting rate.

With equation (5), the field correlation function in equation (15) acquires four contributions,

$$\zeta \langle \mathscr{E}(0)^{(-)} \mathscr{E}(\tau)^{(+)} \rangle = \xi \langle d(0)d^\dagger(\tau) \rangle + \xi |P|^2 \exp{(-2i\bar{\omega}\tau)} \langle d^\dagger(0)d(\tau) \rangle$$
$$- \xi P^* \exp{(-2i\bar{\omega}\tau)} \langle d(0)d(\tau) \rangle - \xi P \langle d^\dagger(0)d^\dagger(\tau) \rangle, \tag{17}$$

where we introduced the parameter

$$\xi = \zeta \left(\frac{\omega_0^2}{4\pi\varepsilon_0 r c^2} \right)^2 |\boldsymbol{\mu}_{eg} \cdot \mathbf{e}_d|^2. \tag{18}$$

The atomic correlation functions in equation (17) can be found by transforming first to the Schrödinger picture. This yields

$$\langle d(0)d^\dagger(\tau) \rangle = \mathrm{Tr} \, d^\dagger \exp{[-i(L_a - i\Gamma)\tau]}(\bar{\rho}d), \tag{19}$$

and similar expressions hold for the other three correlation functions. With the explicit forms of L_a, Γ and $\bar{\rho}$ from section 3, we obtain

$$\langle d(0)d(\tau) \rangle = \langle d^\dagger(0)d^\dagger(\tau) \rangle = 0, \tag{20}$$

$$\langle d(0)d^\dagger(\tau) \rangle = \bar{n}_e \exp{[-i\omega_0\tau - \tfrac{1}{2}(A_e + A_g)\tau]}, \tag{21}$$

$$\langle d^\dagger(0)d(\tau) \rangle = \bar{n}_g \exp{[i\omega_0\tau - \tfrac{1}{2}(A_e + A_g)\tau]}, \tag{22}$$

for $\tau \geqslant 0$. Apparently, the last two terms on the right-hand side of equation (17) vanish.

Combining everything gives for the fluorescence spectrum

$$J(\omega) = \frac{I_e}{\pi} \mathrm{Re} \frac{1}{\tfrac{1}{2}(A_e + A_g) - i(\omega - \omega_0)} + \frac{I_g}{\pi} \mathrm{Re} \frac{1}{\tfrac{1}{2}(A_e + A_g) - i(\omega + \omega_0 - 2\bar{\omega})}, \tag{23}$$

where

$$I_e = \xi \bar{n}_e, \qquad I_g = \xi \bar{n}_g |P|^2. \tag{24}$$

The spectrum $J(\omega)$ is a sum of two Lorentzians, both with a half-width at half-maximum equal to $\tfrac{1}{2}(A_e + A_g) = \tfrac{1}{2}A(1 + |P|^2)$. Similar results were found by Milonni et al. [7] and Gaeta and Boyd [8]. The values of $|P|$ are in the range $0 \leqslant |P| < \infty$. Therefore, the minimum value of the linewidth is $\tfrac{1}{2}A$, and this width grows indefinitely with increasing (intensity) reflection $|P|^2$. The first spectral line on the right-hand side of equation (23) has a strength equal to I_e, and is located at $\omega = \omega_0$. This line is due to the decay process in figure 1 (a). Notice that I_e is proportional to $\bar{n}_e$, as it should be because the initial state is $|e\rangle$. Similarly, the second line has a strength

I_g, and is positioned at $\omega = 2\bar{\omega} - \omega_0$. The responsible process is the three-photon process from figure 1 (*b*). The line strengths as a function of $|P|^2$ are shown in figure 2. Obviously, both I_e and I_g vanish for $|P|^2 \to 0$. For large reflectivity they behave as

$$I_e/\xi \to \tfrac{1}{2}, \qquad I_g/\xi \to \tfrac{1}{2}|P|^2, \tag{25}$$

and it always holds that

$$I_g \geqslant 2I_e, \tag{26}$$

as follows from

$$I_g/I_e = 2 + |P|^2. \tag{27}$$

When we designate photons in the I_e and I_g lines as 'e-photons' and 'g-photons', respectively, equation (26) expresses that there are more than twice as much g-photons than there are e-photons. This can be understood as follows. An e-photon is emitted during ordinary spontaneous decay, and it propagates either in the positive or negative z-direction. Since the detector is located in the region $z > 0$, half the number of e-photons can never reach the detector. They travel towards the surface of the PC, and are subsequently annihilated in a four-wave mixing process inside the medium. The g-photons, on the other hand, always propagate in the positive z-direction. This explains the inequality (26), and the factor of 2. The reason why I_e has an upper limit lies in the fact that the process is ordinary spontaneous decay. When the atom is in $|e\rangle$ at a certain time, it takes a time $1/A$ to decay and to emit the e-photon. Then the atom has to be excited again during a g-photon emission before it can emit a subsequent e-photon. This limits the emission rate to $\tfrac{1}{2}A$ (for the positive z-direction), and the detection rate to $\tfrac{1}{2}\xi$. The three-photon process, however, is brought about by stimulated transitions, and its repetition rate can be enhanced
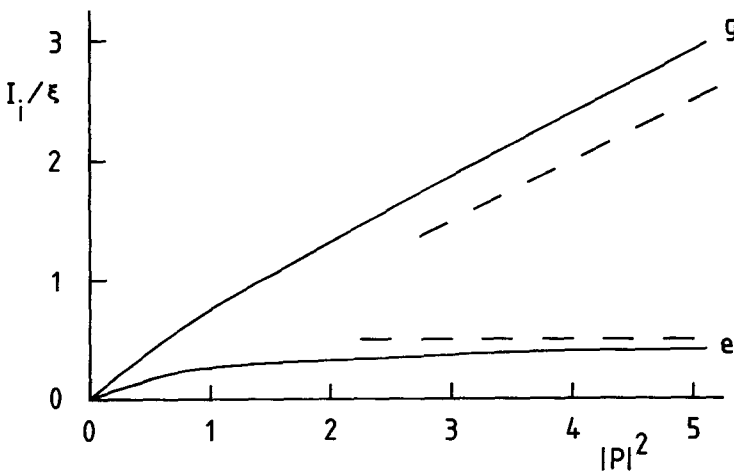

Figure 2. Curves e and g represent the strengths I_e and I_g of the e-line and the g-line, respectively, as a function of the reflectivity $|P|^2$. We have plotted the dimensionless quantities I_e/ξ and I_g/ξ. The dashed lines indicate the asymptotic values ($|P|^2 \to \infty$).
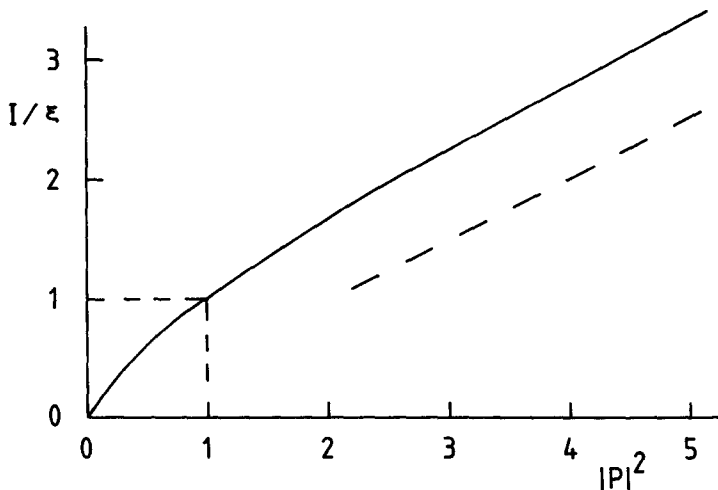
Figure 3.   Plot of the total intensity I (divided by ζ) as a function of $|P|^2$. The dashed line, at $I/\zeta = \frac{1}{2}|P|^2$, is the asymptotic limit.

unlimitedly by increasing the strength of the 'external field' ($\bar{\omega}$-photons).

The spectrally unresolved emission rate is found to be

$$I = I_e + I_g = \tfrac{1}{2}\zeta |P|^2 \frac{3 + |P|^2}{1 + |P|^2},$$ (28)

and its dependence on $|P|^2$ is illustrated in figure 3.

5. Photon correlations

The temporal characteristics of the fluorescent photons are most conveniently expressed in terms of the two-photon correlation function $I_2(t_1, t_2)$. By definition, $I_2(t_1, t_2)\, dt_1\, dt_2$ equals the probability for the detection of a photon in $[t_1, t_1 + dt_1]$, together with the detection of a photon in $[t_2, t_2 + dt_2]$, but independent of detections at other times. The photon correlation function can be expressed in terms of the incident field on the photomultiplier, according to [9, 10]

$$I_2(t_1, t_2) = \zeta^2 \langle \mathscr{E}(t_1)^{(-)} \mathscr{E}(t_2)^{(-)} \mathscr{E}(t_2)^{(+)} \mathscr{E}(t_1)^{(+)} \rangle,$$ (29)

for $t_2 \geqslant t_1$. When the atom is in the steady state $\bar{\rho}$, then $I_2(t_1, t_2)$ depends only on t_1 and t_2 through $t_2 - t_1$, as can be checked by inspection. Therefore, we shall only consider $I_2(0, \tau)$, with $\tau \geqslant 0$.

With expression (5) for $\mathscr{E}(t)^{(+)}$, we can work out the right-hand side of equation (29) and express $I_2(0, \tau)$ in terms of atomic correlation functions. Due to the special form of $\bar{\rho}$, many of these correlation functions turn out to be zero (as in equation (20)). It appears that $I_2(0, \tau)$ consists of four terms and can be written as

$$I_2(0, \tau) = \sum_{\alpha\beta} f_{\beta\alpha}(\tau) I_\alpha.$$ (30)

where the summation runs over $\alpha = e$, g and $\beta = e$, g. The intensities I_e and I_g are again the intensities of the e-line and the g-line, respectively, and the functions $f_{\beta\alpha}(\tau)$ are defined as

$$f_{\alpha\beta}(\tau) = \frac{1}{I_\alpha} \zeta^2 \mathrm{Tr}\, R_\beta \exp(-iL\tau) R_\alpha \bar{\rho}, \qquad (31)$$

with $L = L_a - i\Gamma$. The Liouville operators R_e and R_g are

$$R_e \sigma = d^\dagger \sigma d = P_g \langle e|\sigma|e \rangle, \qquad (32)$$

$$R_g \sigma = |P|^2 d\sigma d^\dagger = |P|^2 P_e \langle g|\sigma|g \rangle, \qquad (33)$$

for an arbitrary σ. From equation (30) and the definition of $I_2(0, \tau)$, it follows that $f_{\beta\alpha}(\tau) I_\alpha$ equals the probability for the detection of a β-photon at time $t = \tau$ and an α-photon at time $t = 0$. Therefore, $f_{\beta\alpha}(\tau)\,\mathrm{d}\tau$ has the significance of the probability for the detection of a β-photon at time τ after the detection of an α-photon at time zero. With the properties

$$\lim_{\tau \to \infty} \exp(-iL\tau)\sigma = \bar{\rho}\, \mathrm{Tr}\, \sigma, \qquad (34)$$

$$\zeta\, \mathrm{Tr}\, R_\alpha \bar{\rho} = I_\alpha, \qquad (35)$$

which can be verified easily, we find from equation (31)

$$\lim_{\tau \to \infty} f_{\beta\alpha}(\tau) = I_\beta. \qquad (36)$$

This relation expresses that for a long delay time τ, the detection of the β-photon becomes independent of the detection of the α-photon. Combination of equations (30) and (36) gives

$$I_2(0, \infty) = \sum_{\alpha\beta} I_\beta I_\alpha = I^2, \qquad (37)$$

where $I = I_e + I_g$ is the uncorrelated intensity.

The operator R_α can be viewed as the emission operator for an α-photon. Equation (35) expresses that the detection rate I_α for α-photons equals ζ times the expectation value of the operator R_α. The parameter ζ relates the emission rate to the detection rate. This picture is also supported by equation (31). Reading from right to left, the atom is initially in state $\bar{\rho}$. The action of R_α then corresponds to the emission of the α-photon. Subsequently, the atomic state evolves over a time τ with $\exp(-iL\tau)$, after which the action of R_β causes the emission of the β-photon. The factor ζ^2 relates the two emission rates to detection rates. Finally equations (32) and (33) show explicitly the effect of the action of an emission operator on an atomic density operator. Action of R_e on σ leaves the atom in the ground state, as represented by the projector P_g on $|g\rangle$, and generates the factor $\langle e|\sigma|e\rangle$ which is the population of the excited state. This is precisely what happens in figure 1 (*a*). The probability for the emission of an e-photon is proportional to the population of $|e\rangle$, since the atom must be initially in the excited state, and after the emission the atom is in the ground state. Similarly, the action of R_g leaves the atom in $|e\rangle$, and the probability for the emission of a g-photon is proportional to $\langle g|\sigma|g\rangle$, as expressed by equation (33). This interpretation is consistent with the processes in figure 1 (*b*).

Of particular interest is the behaviour of $f_{\beta\alpha}(\tau)$ for small values of τ. When $f_{\beta\alpha}(0) > I_{\beta}$, then the emission of the α-photon enhances the probability for the emission of the subsequent β-photon, as compared to the uncorrelated probability for the emission of a β-photon. When $f_{\beta\alpha}(0) < I_{\beta}$, then the α-emission reduces the probability for a β-emission. With

$$R_e^2 = R_g^2 = 0, \tag{38}$$

as follows from equations (32) and (33), we find

$$f_{ee}(0) = f_{gg}(0) = 0. \tag{39}$$

The relation $f_{ee}(0) = 0$ expresses that the probability for the emission of an e-photon, immediately following an e-emission, is zero. This should be so, because after the emission of the first e-photon the atom is in its ground state, and subsequent emission of an e-photon requires that the atom is in the excited state. This necessary $|g\rangle \to |e\rangle$ transition is brought about by a three-photon process, which takes a finite time. A similar explanation holds $f_{gg}(0) = 0$.

For the other two correlation functions, we find

$$\frac{f_{eg}(0)}{I_e} = \frac{1}{\bar{n}_e} > 2, \tag{40}$$

$$\frac{f_{ge}(0)}{I_g} = \frac{1}{\bar{n}_g} \geqslant 1, \tag{41}$$

showing that the emission of an e(g)-photon enhances the probability for the emission of a g(e)-photon. This is also easily understood. The probability for an e-emission is proportional to the population of $|e\rangle$. For the uncorrelated emission, the atom is in the steady state $\bar{\rho}$, and the population $\bar{n}_e$ is smaller than unity (and, in fact, smaller than 1/2). After a g-emission, however, the atom is in its excited state with certainty. This explains equation (40), and a similar interpretation can be given to equation (41).
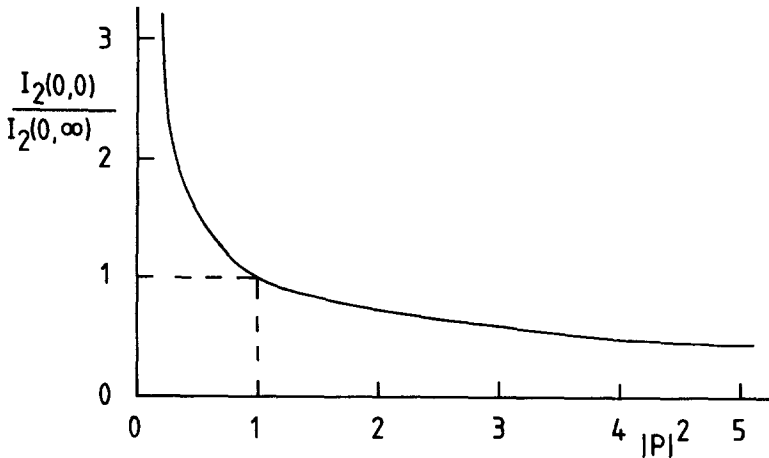

Figure 4.   Photon correlation function for $\tau = 0$, relative to its value for $\tau = \infty$, as a function of $|P|^2$. For $|P|^2 > 1$ the value of $I_2(0, 0)$ is smaller than $I_2(0, \infty)$, which reflects antibunching of photons.
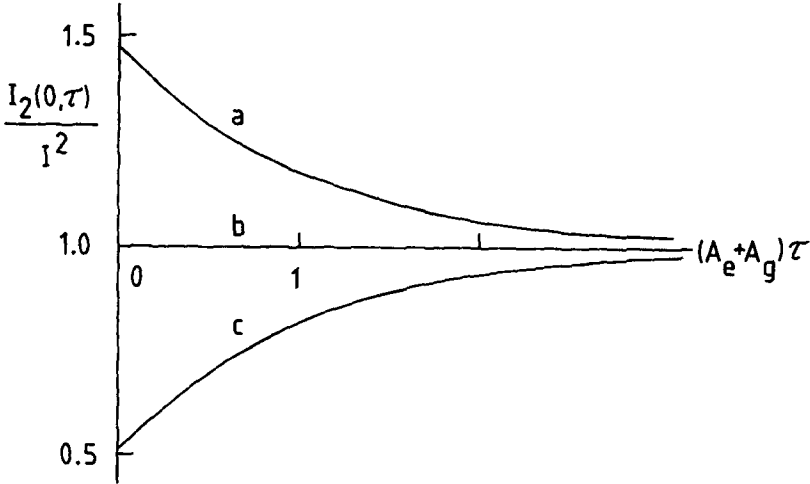
Figure 5.   Curves *a*, *b* and *c* give $I_2(0, \tau)/I^2$ as a function of $(A_e + A_g)\tau$ for $|P|^2 = 0.5$, $|P|^2 = 1$ and $|P|^2 = 4$, respectively. For $|P|^2 = 1$ we have $I_2(0, \tau) = I^2$ for all τ, corresponding to perfectly random (Poisson) detection statistics.

When we do not distinguish between e-photons and g-photons, then we have to consider $I_2(0, \tau)$. For $\tau = 0$ we obtain

$$\frac{I_2(0, 0)}{I_2(0, \infty)} = \frac{4}{x}\left(\frac{1+x}{3+x}\right)^2, \qquad x = |P|^2, \qquad (42)$$

and the corresponding parameter-free curve is shown in figure 4. For $0 < |P|^2 < 1$ we have $I_2(0, 0) > I_2(0, \infty)$, which means that the emission of the first photon enhances the probability for the emission of a second photon. This behaviour is called 'bunching', indicating that photons tend to stick together. Antibunching $(I_2(0, 0) < I_2(0, \infty))$ occurs for $|P|^2 > 1$. The function $I_2(0, \tau)$ is easily calculated, with the result

$$\frac{I_2(0, \tau)}{I^2} = 1 + g(|P|^2) \exp\left[-(A_e + A_g)\tau\right], \qquad (43)$$

where

$$g(x) = (1 - x)\frac{x^2 + 3x + 4}{x(x+3)^2}. \qquad (44)$$

This correlation function is shown in figure 5 for three values of $|P|^2$.

6.   Photon statistics
Photon antibunching is a pure quantum feature of radiation, since it cannot be produced by any classical field [11]. A related phenomenon is the possibility that quantum radiation has sub-Poissonian photon statistics. This means that the variance $\sigma(t)^2$ in the number of detected photons in $[0, t]$ is smaller than the average $\mu(t)$, which never occurs for classical fields. Mandel introduced the Q-factor [12]

$$Q(t) = \frac{\sigma(t)^2 - \mu(t)}{\mu(t)}, \qquad (45)$$

which is negative for sub-Poissonian photon statistics. Negative values of $Q(t)$ have been found experimentally in resonance fluorescence [13, 14]. For stationary radiation the average is $\mu(t) = It$, with I the intensity. The variance can be expressed in $I_2(0, t)$, and the Q-factor is

$$Q(t) = \frac{2}{It} \int_0^t d\tau \{(t - \tau)I_2(0, \tau) - \tau I^2\}. \tag{46}$$

With equation (43) we find for the present problem

$$Q(t) = \frac{2Ig(|P|^2)}{(A_e + A_g)^2 t} \{(A_e + A_g)t - 1 + \exp[-(A_e + A_g)t]\}. \tag{47}$$

The sign of $Q(t)$ is given by the sign of $g(|P|^2)$. Therefore, for $|P|^2 > 1$ we have $Q(t) < 0$ for all t, and the statistics are sub-Poissonian. For small t we find

$$Q(t) = Itg(|P|^2), \qquad t \to 0, \tag{48}$$

showing that $Q(t)$ increases or decreases linearly with t. For $t \to \infty$, $Q(t)$ reaches the stationary value

$$\bar{Q} = \lim_{t \to \infty} Q(t) = \frac{2Ig(|P|^2)}{A_e + A_g}. \tag{49}$$

Recalling that I, A_e and A_g depend on $|P|^2$, we can write for the $|P|^2$ dependence of $\bar{Q}$

$$\bar{Q} = \frac{\xi}{A} \frac{1 - x}{(1 + x)^2} \frac{x^2 + 3x + 4}{x + 3}, \qquad x = |P|^2. \tag{50}$$

The factor ξ/A is an efficiency factor. We see that $\bar{Q} = (\xi/A)(4/3)$ for $|P|^2 \to 0$, $\bar{Q} = 0$ for $|P|^2 = 1$, and $\bar{Q} \to -(\xi/A)$ for $|P|^2 \to \infty$. In view of equation (45), the value of $Q(t)$ is limited by $Q(t) \geqslant -1$ for any field. The lower limit $Q(t) = -1$ corresponds to $\sigma(t)^2 = 0$, which is the ultimate sub-Poissonian limit. By increasing the phase-conjugate reflectivity $|P|^2$, this lower limit can be approached arbitrarily closely, apart from the efficiency factor ξ/A. The dependence of $\bar{Q}A/\xi$ on $|P|^2$ is shown in figure 6.
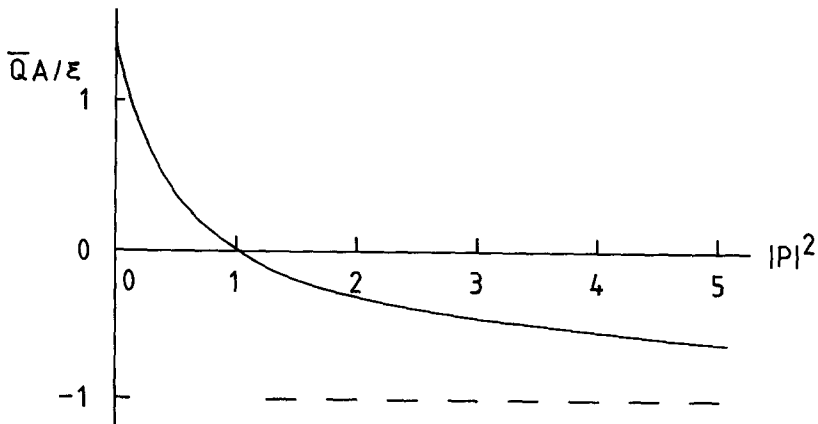

Figure 6.   Plot of the normalized $\bar{Q}$-factor, $\bar{Q}A/\xi$, as a function of $|P|^2$. For $|P|^2 = 1$ we have $\bar{Q} = 0$, which reflects uncorrelated photon statistics. The dashed line at $\bar{Q}A/\xi = -1$ is the asymptotic limit.

7. Conclusions

We have studied the spectral and temporal properties of fluorescence radiation, which is emitted by an atom near the surface of a PC. The fluorescence spectrum was found to be the sum of two Lorentzians, and the positions of the lines appeared to be consistent with the two relaxation processes shown in figure 1. Three-photon processes contribute more than twice as much to the fluorescence yield compared with ordinary spontaneous decay. From the result for the two-photon correlation function $I_2(0, \tau)$, it followed that the fluorescent photons exhibit antibunching when the reflectivity of the PC exceeds unity. Under the same criterion, the photon statistics are sub-Poissonian.

Acknowledgment

References

[1] GAETA, A. L., and BOYD, R. W., 1988, *Phys. Rev. Lett.*, **60**, 2618.
[2] COOK, R. J., and MILONNI, P. W., 1988, *IEEE J. quant. Electron*, **24**, 1383.
[3] HENDRIKS, B. H. W., and NIENHUIS, G., 1989, *Phys. Rev.* A, **40**, 1892.
[4] COHEN-TANNOUDJI, C., 1977, *Frontiers in Laser Spectroscopy*, Proc. 27th Les Houches Summer School, edited by R. Balian, S. Haroche, and S. Liberman (Amsterdam: North Holland).
[5] ARNOLDUS, H. F., and GEORGE, T. F., 1991, *Phys. Rev.* A, **43**, 3675.
[6] ARNOLDUS, H. F., and GEORGE, T. F., 1991, *Phys. Rev.* A (in press).
[7] MILONNI, P. W., BOCHOVE, E. J., and COOK, R. J., 1989, *J. opt. Soc. Am.* B, **6**, 1932.
[8] GAETA, A. L., and BOYD, R. W., 1990, *Coherence and Quantum Optics VI*, edited by J. H. Eberly, L. Mandel, and E. Wolf (New York: Plenum), p. 343.
[9] GLAUBER, R. J., 1965, *Quantum Optics and Electronics*, edited by C. DeWitt, A. Blandin and C. Cohen-Tannoudji (New York: Gordon and Breach), p. 63.
[10] KELLEY, P. L., and KLEINER, W. H., 1964, *Phys. Rev.*, **136**, A316.
[11] PAUL, H., 1982, *Rev. mod. Phys.*, **54**, 1061.
[12] MANDEL, L., 1979, *Optics Lett.*, **4**, 205.
[13] SHORT, R., and MANDEL, L., 1983, *Phys. Rev. Lett.*, **51**, 384.
[14] REMPE, G., SCHMIDT- KALER, F., and WALTHER, H., 1990, *Phys. Rev. Lett.*, **64**, 2783.